Clinical Spectroscopy 5 (2023) 100029

Contents lists available at ScienceDirect

Clinical Spectroscopy

journal homepage: www.sciencedirect.com/journal/clinical-spectroscopy

Rapid detection of heart failure using a spectroscopic liquid biopsy

Loren Christie [a,b], Alexandra Sala [a], James M. Cameron [a], Justin J.A. Conn [a], David S. Palmer [a,b], William J. McGeown [d], Jane A. Cannon [e], John Sharp [f], Matthew J. Baker [a,c,*,1]

[a] Dxcover Ltd, Royal College Building, 204 George Street, Glasgow G1 1XW, UK
[b] Department of Pure and Applied Chemistry, University of Strathclyde, Thomas Graham Building, 295 Cathedral Street, Glasgow G1 1XL, UK
[c] School of Medicine, Faculty of Clinical and Biomedical Sciences, University of Central Lancashire, Preston PR1 2HE, UK
[d] Department of Psychological Sciences and Health, University of Strathclyde, Graham Hills Building, 40 George Street, Glasgow G1 1QE, UK
[e] BHF Cardiovascular Research Centre, University of Glasgow, 126 University Place, Glasgow G12 8TA, UK
[f] Consultant Clinical Psychologist, Scottish National Advanced Heart Failure Service, Golden Jubilee National Hospital, Glasgow, UK

ARTICLE INFO

Keywords:
FTIR
Spectroscopic Liquid Biopsy
Heart Failure
Clinical Spectroscopy
Vibrational spectroscopy
Novel FTIR

ABSTRACT

Heart disease is growing annually across the globe with numbers expected to rise to 46% of the population by 2030. Early detection is vital for several reasons, firstly it improves the long-term prognosis of the patient by admitting them through the appropriate pathway faster, secondly it reduces healthcare costs by streamlining diagnosis and finally, in combination with management or treatment, it can prevent the progression of the disease which in turn improves the patient's quality of life. Therefore, there lies an increasing need to develop assays which can rapidly detect heart disease at an early stage. The Dxcover® liquid biopsy platform employs infrared spectroscopy and artificial intelligence, to quickly analyse minute amounts of patient serum. In this study, discrimination between healthy controls and diseased patients was obtained with an area under the receiver operating characteristic curve (AUC) of 0.89. When assessing the heart failure vs all patients, which is most akin to what would be observed in a triage setting, the model when tuned to a minimum of 45% specificity yielded a sensitivity of 89% and an NPV of 0.996, conversely when sensitivity was set at a 45% minimum, the specificity was 96%, giving an NPV of 0.991 when using a 1.5% prevalence. Other models were assessed in parallel, but the performance of the ORFPLS model was overall superior to the other models tested. In this large scale (n = 404) proof-of-concept study, we have shown that the Dxcover liquid biopsy platform has the potential to be a viable triage tool in emergency and routine situations for the diagnosis of heart failure.

1. Introduction

Cardiovascular diseases (CVDs) are the main cause of death worldwide. According to the World Health Organisation (WHO), almost 18 million people die of CVDs every year, accounting for the 32% of all global deaths; moreover, cases are expected to rise to 46% of the population by 2030 [1,2]. Coronary artery disease (CAD), also called coronary heart disease (CHD) or ischaemic heart disease, occurs when atherosclerotic plaques (i.e., fatty deposits) block or temporarily interrupt the heart's blood supply [3,4]. CAD is a major cause of more severe heart conditions, such as myocardial infarction (MI; i.e., heart attack), heart failure (HF), and atrial fibrillation (AF). A myocardial infarction occurs when there is a blockage to one or more of the coronary arteries which supply blood to the heart muscle. When a MI occurs the affected area of the heart muscle can become damaged or die which can lead to chest pain, shortness of breath and if left untreated a fatal heart attack. AF is a type of abnormal heart rhythm specifically in the upper chambers of the heart. It can cause blood to pool in the atria instead of being pumped around all chambers.

HF is described as the general inability of the heart to pump the

Abbreviations: AI, artificial intelligence; AF, atrial fibrillation; AUC, area under the ROC curve; CAD, coronary artery disease; CHD, coronary heart disease; CT, computer tomography; CVD, cardiovascular disease; ECG, electrocardiogram; HF, heart failure; ICM, ischaemic cardiomyopathy; MI, myocardial infarction; ML, machine learning; MRI, magnetic resonance imaging; NICM, non-ischaemic cardiomyopathy; ORFPLS, oblique random forest partial least squares; PLS-DA, partial least squares-discriminant analysis; RF, random forest; ROC, receiver operating characteristic; SVM, support vector machine.

* Corresponding author at: Dxcover Ltd, Royal College Building, 204 George Street, Glasgow G1 1XW, UK.
E-mail addresses: matthew.baker@dxcover.com, mbaker10@uclan.ac.uk (M.J. Baker).
[1] Twitter: @ChemistryBaker – @dxcover.

https://doi.org/10.1016/j.clispe.2023.100029
Received 27 July 2023; Received in revised form 18 October 2023; Accepted 20 October 2023
Available online 21 October 2023

blood around the body; it can be acute or chronic and tends to worsen over time if it is not diagnosed in a timely manner and symptoms are not controlled [5]. HF and AF can also develop without the presence of CAD, arising from hypertension (i.e. high blood pressure) or congenital heart diseases [4–6].

There are two common types of heart failure: ischemic cardiomyopathy (ISCM) and non-ischemic cardiomyopathy (NISCM). The former describes the condition whereby the heart is ineffective at pumping blood around the body; this can be due to comorbidities such as CAD or any sort of increase of plaque in the arteries which restricts blood flow. The latter, NISCM, is not as widely understood and can result from a number of sources such as genetic factors or auto-immune diseases. It can also vary significantly between populations, socioeconomic groups and geographical areas [7,8].

HF is currently diagnosed using an echocardiogram (EGC) or medical imaging (e.g. chest X-ray), while CAD may also involve coronary angiography, magnetic resonance imaging (MRI) and/or computerised tomography (CT) investigations [9,10]. Prior to further diagnostics, a preliminary blood test is conducted, which assesses the levels of N terminal pro-brain natriuretic peptide (NTproBNP) within the patient's blood plasma [11]. This peptide hormone is released upon stretching of the heart walls or when the heart is under significant duress, it has a variable negative predictive value (NPV) between 0.88 and 0.98 depending on the demographic and the concentration threshold of peptide found in the blood [12]. The benefits of this assay are similar to the Dxcover infrared assay, being non-invasive and can provide rapid, accurate results [13]. The issues however, are that this type of testing has reduced sensitivity at higher peptide concentration thresholds, it can be difficult to acquire and it is not specific to heart failure and other diseases such as respiratory failure, pulmonary embolism or chronic kidney disease may artificially inflate the peptide levels [9,12]. The spectroscopic liquid biopsy method could provide an alternative to this blood test and aid in the triage of heart failure.

Using isolated ECG results is not a definitive method for diagnosing heart failure and as such another test must be used in conjunction to increase the diagnostic performance. Additionally, ECG results must be interpreted by a GP, which can introduce a level of subjectivity and eventually lead to further diagnostic uncertainty.

Despite the use of these technologies, HF and CAD are not easily diagnosed due to their complex symptomologies and somewhat vague presentations such as breathlessness or fatigue, making specific diagnoses difficult. In the first stages of HF, the pathology can develop with no symptoms at all or showing only minor symptoms when induced by physical activity. CAD presents with similar symptoms to HF, or presents itself with angina (i.e., chest pain) and/or heart attack [9,14]. Furthermore, angiography is a costly and invasive diagnostic method which could lead to various severe complications, such as artery dissection, and fatalities have also been reported [15]. Thus, a reliable, low-cost, and minimally invasive blood test that can quickly detect HF would be beneficial as an alternative or additional test, particularly where the uptake of the NTproBNP testing is not routine or can have a lengthy turnaround time. Furthermore, a rapid triage test would be of great value in emergency situations where a fast diagnosis is vital.

Artificial intelligence (AI) and machine learning (ML) algorithms have gained interest in the diagnostics field for the classification of different pathologies, including CAD diagnosis [15–17]. In the past few decades, the clinical utility of infrared (IR) spectroscopy has been investigated for disease diagnostics in several fields, such as cancer research, infectious disease discovery and the early detection of Alzheimer's [18,19]. In Biofluid spectroscopy has attracted the attention of many researchers because of the ease of sample collection and handling, combined with a minimal sample preparation [20]. Human blood serum contains over 20,000 different proteins and gains proteomes from surrounding tissues and cells of the entire body; hence, it presents itself as a powerful clinical tool for its concentration of various biomarkers and diagnostic indicators of many pathologies [20].

Attenuated total reflection Fourier transform infrared (ATR-FTIR) spectroscopy has already been shown to be well-suited to current clinical diagnostic pathways, not only for the reproducibility, but also for being cost-effective and easy to use. When coupled with machine learning, the technique has the potential to differentiate between disease classes [20–22].

In this study, we employed the Dxcover® liquid biopsy platform to primarily discriminate between patients suffering from HF including ISCM, NISCM and AF (i) vs healthy controls and (ii) vs symptomatic patients (those with known coronary heart disease but not heart failure); patients suffering from HF with NISM and AF (iii) vs healthy controls and (iv) vs symptomatic patients; (v) HF including ISCM, NISCM and AF vs healthy controls and symptomatic patients together, Table 1 summarises these classes. The Dxcover approach can cut down on the sample processing, preparation and analysis time compared to the NTproBNP method which utilises an electrochemiluminescence immunoassay (ECLIA) this also requires expensive equipment, reagents and a specialised setup.

The aim of this feasibility study was to determine whether the Dxcover liquid biopsy platform could be utilised to identify patients with heart failure and discriminate between them and healthy controls as well as symptomatic patients in order to be considered viable as an alternative heart failure triage method.

2. Materials and methods

2.1. Sample collection

The patient sample cohort consisted of 147 healthy controls (with no history of coronary artery disease, heart failure, or any other chronic illness, and they were not on any regular medication), 61 cardiac control patients determined to be Class I/Stage A according to the New York Heart Association (NYHA) functional classification (known coronary artery disease with no heart failure and in sinus rhythm), 51 patients with heart failure and non-ischaemic cardiomyopathy (termed as HFNOCAD for this analysis, included patients with known heart failure but no history of coronary artery disease), 75 patients with heart failure and atrial fibrillation (patients exhibiting atrial fibrillation with a known history of heart failure) and 70 patients with heart failure and ischaemic cardiomyopathy (in sinus rhythm). Table 1 details the patient groupings associated with each classification. The patients were grouped in such a way as the purpose of this work was to broadly identify and classify heart failure patients versus healthy or symptomatic controls.

Blood samples were collected at the Clinical Research Unit at the British Heart Foundation Glasgow Cardiovascular Research Centre (GCRC; Western Infirmary, Glasgow, UK), using a gold top BD vacutainer tube (BD, USA) containing a clot activator and serum separating gel, samples were then centrifuged to separate the red blood cells from the serum component. The serum was then aliquoted into several cryotubes and stored at − 80 °C. Further information about the ethics approval can be found in the supplementary information.

Table 1
Each classification problem and details on patient symptomology.

Classification problem	Description
(i) HF vs HEALTHY	HF including ISCM, NISCM and AF vs Healthy controls
(i) HF vs SC	HF including ISCM, NISCM and AF vs Symptomatic patients
(i) HFNOCAD vs HEALTHY	HF including NISCM and AF vs Healthy controls
(i) HFNOCAD vs SC	Hf including NISCM and AF vs Symptomatic patients
(v) HF vs ALL PATIENTS	HF including ISCM, NISCM and AF vs Healthy controls and symptomatic patients

2.2. Sample preparation

All serum samples were thawed at room temperature for 20 min. For each patient, 3 μL of serum was pipetted onto each of the three sample wells of a Dxcover® Sample Slide (Dxcover Ltd., UK), using a total of 9 μL per patient. The prepared slides were then placed into a drying unit incubator (Thermo Fisher ™ Heratherm ™, GE) at 35 °C for one hour to control the drying dynamics of the serum droplets.

2.3. Data collection

The IR spectra were collected using a PerkinElmer Spectrum 2 FTIR spectrometer (PerkinElmer, UK) fitted with a Dxcover® Autosampler (Dxcover Ltd., UK). The spectral parameters used for acquisition were as follows; a range of 4000–450 cm^{-1}, a resolution of 4 cm^{-1} and 16 co-added scans. A background measurement of the specified background well was taken prior to each sample analysis. The background measurement is automatically subtracted from the sample spectra in order to account for environmental differences. Three replicates of each of the three sample wells were taken yielding a total of nine spectra per patient.

2.4. Data analysis: pre-processing and classification

Several spectral pre-processing methods were examined to assess their influence on the area under the receiver operating characteristic (ROC) curve (AUC) value for each classification. These included an Extended Multiplicative Signal Correction (EMSC), reducing the spectral range, normalisations, and finally a binning which reduces the resolution and smooths the spectra. These were all applied using the PRFFECTv3 software within the R Studio environment [23]. The pre-processing parameters used were different combinations for each classification problem, and are summarised in Table 2.

Mean spectral plots were created for each disease class, and principal component analysis (PCA) was carried out to generate PCA scores plots and the corresponding loadings, which can highlight differences within datasets.

Several models were investigated for their performance including support vector machine (SVM), partial least squares (PLS) and random forest (RF) and oblique-random forest partial least squares (ORFPLS). The ML algorithms were trained using a nested cross validation strategy. The patients were randomly split into a training (70%) and a test (30%) set. Model hyperparameters were selected by a grid search to optimize AUC for 5-fold cross-validation on the training set. Subsequently, the whole procedure was repeated 51 times using different training and test sets as this was determined to be the optimum number of resamples to maximise the AUC results. On each repeat, the model was trained on the training set and used to make predictions of the test set to assess the predictive performance. The statistics reported below are averages of the statistics obtained on each of the 51 test sets.

Table 2
Preprocessing strategies applied to each classification problem to yield the highest area under the receiver operating curve (AUC).

Classification	Pre-processing
(i) HF vs Healthy	Cut (1000–3700 cm^{-1}), EMSC, Min-max Normalisation, Binning of 4, Remove (1801–2799 cm^{-1})
(i) HF vs SC	Cut (1000–1800 cm^{-1}), EMSC, Vector Normalisation
(i) HFNOCAD vs Healthy	Cut (1000–3700 cm^{-1}), EMSC, Min-max Normalisation, Remove (1801–2799 cm^{-1})
(i) HFNOCAD vs SC	Cut (1000–1800 cm^{-1}), EMSC, Vector Normalisation, Binning of 8
(v) HF vs Healthy and SC	Cut (1000–3700 cm^{-1}, EMSC, Min-max Normalisation, Binning of 4, Remove (1801–2799 cm^{-1})

3. Results and discussion

3.1. PCA overview

The data was first investigated for patterns and significant outliers using PCA. All classes were projected into the PC space to distinguish any obvious differences between each of the classes. Firstly, Fig. 1 shows the mean spectra for all classes after pre-processing; the spectra were reduced to 3500 – 1000 cm^{-1} and EMSC was applied.

The mean spectra for all classes overall appear very similar, but clear differences are evident within certain spectral areas, such as the lipid peak at 1740 and 2800 cm^{-1} and the dip between the two amide peaks at 1650 and 1540 cm^{-1}. The PCA plot generated was investigated next to assess whether these spectral differences could differentiate classes from one another. Fig. 2 shows the overall PCA score plot along with the densities and PCs 1–4.

To meet the needs of this study, the groups have been combined for some machine learning analyses as detailed in the introduction. For instance, groups 1–2–5 can be grouped into one heart failure (HF) category and groups 2 and 5 can be grouped into HF without any associated coronary artery disease (HFNOCAD), or in other words, heart failure with non-ischaemic cardiomyopathy. Table 1 in Section 2.1 further describes these groupings. No obvious splits or clustering of classes can be observed in the PCA scores plots and the density plots overlap substantially (Fig. 2) suggesting supervised machine learning methods are required to extract the differences between disease groups.

3.2. ROC overview

A variety of ML models were applied to assess their ability to differentiate between disease classes. The AUCs were computed for each model type (i.e. PLS, RF, SVM and ORFPLS) based on 51 resamples and can be found in Tables 1–5 in the supplementary information. The best performing model based on the highest AUC of all classification types was the ORFPLS, for which results can be found in Table 3 below. The optimum preprocessing that was applied for this model differs between each classification due to different regions of the spectra being considered more important diagnostically than others. The diagnostically significant peaks can differ between each classification problem, and therefore require different preprocessing approaches to more easily highlight the small changes between classes. The breakdown of which strategies were utilised can be found in Table 2.

Receiver operating characteristic (ROC) curves were created to assess model performance. Each classification has its own separate curve as plotted in Fig. 3. The AUC values are slightly different to those stated in the above table as they are calculated differently, the figure shows the AUC of the mean ROC curve across all 51 resamples, whereas the results in Table 3 show the mean of all AUCs across all resamples. The closer the value is to 1, the better the model is at discriminating between classes. The HF vs healthy problem yields the highest AUC as determined by the ORFPLS model (0.89). The model does not perform as well when attempting to distinguish between symptomatic controls, this could be due to the body responding similarly to a patient who has heart failure and a patient who has a condition such as hypertension for example, leading to similar signatures being picked up within the spectra.

As well as determining the highest AUC values, the ORFPLS model was also tuned to 90% sensitivity and specificity respectively to assess the corresponding sensitivity or specificity when the other metric is set to a high threshold, these values are plotted in Table 4. This can also aid in comparisons to other techniques which may have values within this range. Points along the ROC curve can be selected to assess the value of sensitivity or specificity and its corresponding counterpart at that point. This is useful as clinical requirements can vary and so any point can be picked along the curve that matches what is required (screening or diagnostic tool). For example a 45% minimum threshold for specificity has been cited in previous studies involving liquid biopsies [24,25]. The

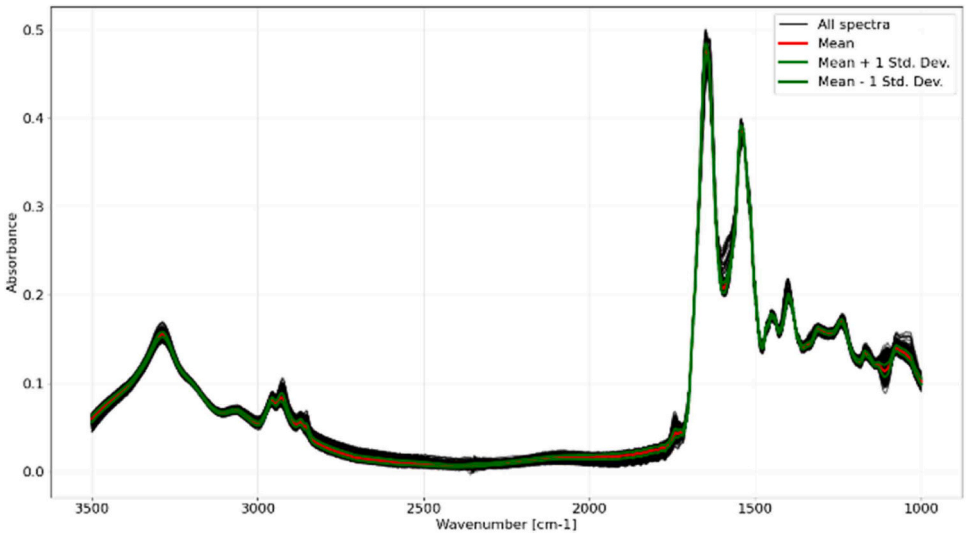

Fig. 1. Overall mean spectra for all five subclasses, including + /− 1 standard deviations.

sensitivities and specificities were recomputed based on either the corresponding sensitivity or specificity being set at a 45% minimum, Table 5 details these results.

The results gained when setting the minimum metric to at least 45% appears to provide a more clinically viable overall result when considering the implementation of this as a triage tool as opposed to aiming for the highest possible sensitivity or specificity, as the counterpart value decreases sharply when the metric is > 90%. For HF vs healthy and symptomatic patients, which most mimics what would be observed in a triage setting, when the sensitivity is set to a minimum of 45% the specificity is 96%, the corresponding NPV would therefore be 0.991 when the prevalence is assumed to be 1.5% in accordance to the trend in the general population of all European adults [26]. Alternatively, when aiming for a minimum of 45% specificity, the model gives a sensitivity of 89% and an NPV of 0.996. Both 45% minimum tuned models provide an excellent NPV which surpasses the current peptide blood test NPV metric but is slightly less in overall sensitivity when tuned to 45% specificity. Therefore, the model used can be chosen depending on clinical requirements, be they as a screening tool (higher sensitivity) or a diagnostic tool (higher specificity). A range of prevalences were also investigated to better capture the increase in prevalence upon increasing age and the associated NPVs, these results can be seen in Table 6.

The NPV, sensitivity and specificity of the currently used NT-proBNP assay can vary depending on the range of the protein within the blood (at higher concentrations the sensitivity of the assay decreases) as well as the age of patient. These values can range between 0.88 and 0.98 for the NPV, 90% and 99% for the sensitivity and 43% and 76% for the specificity [12].

3.3. Feature importance

A feature importance plot was generated for each classification using the ORFPLS model and can be seen in Fig. 4. These show the regions/wavenumbers within the spectrum that are deemed the most important for discriminating between classes.

When assessing the discrimination ability of the model to distinguish between HF against healthy patients, important regions were discovered across the full spectrum, from 3700 to 1000 cm^{-1}. At the higher wavenumber region, a common important feature is the lipid peak between 2900 and 2800 cm^{-1}. Lipid regions being determined as diagnostically important is a common theme throughout all classifications here; this could be due to heart diseases being intrinsically correlated with high levels of cholesterol or fat within the blood and as such, this region is determined as diagnostically significant when attempting to detect heart failure [28]. This hypothesis is supported by the fact that when classifying against heart failure patients with no coronary heart disease the lipid regions appear less important, and different biomolecules are deemed more important for this problem.

For the classifications versus symptomatic patients, the optimum preprocessing cut the spectra to the fingerprint region (1800–1000 cm^{-1}) as the most important discriminators were found to be located within this section. There is a peak in common for both of HF and HFNOCAD vs SC at around 1400 cm^{-1} which can be attributed to lipids/fatty acids.

Interestingly, for HF vs healthy and symptomatic patients, the amide I peak and falling edge at 1640 cm^{-1} appear prominent in the importance plot. This could be due to the influence of combining healthy and symptomatic patients causing this particular area to be of compounded importance as opposed to the lipid peaks, which are still defined as important regions, particularly the 2800 cm^{-1} peak which is comparable to its neighbouring amide A peak at ~3300 cm^{-1}. Amide peaks are one of the largest within a serum spectrum and are often found to be of diagnostic significance as they relate to vibrations within protein molecules which have been shown to be suggestive of disease state [29].

3.4. Summary

Implementation of the Dxcover infrared spectroscopic liquid biopsy could aid in the triage of heart failure as a bench top system that requires only a blood draw from a patient. This is a rapid test which can yield results in just 15 min as opposed to currently used methods which can have a longer turnaround time as well as specialist personnel. Blood serum testing is already performed routinely within medical settings and as such the pathway already exists for a liquid spectroscopic biopsy to inhabit this space. The most widely used blood test (NT-proBNP) yields an NPV of between 0.88 and 0.98, a sensitivity of between 90% and 99% and a specificity between 43% and 76%, depending on the concentration threshold (sensitivity worsens as peptide concentration in the blood increases) [12]. The Dxcover liquid biopsy gives an NPV of between 0.97 and 0.99 at a specificity of 45% and sensitivity of 89% or when tuned to 45% sensitivity, specificity is 96% and NPV is between 0.94 and 0.99. The true advantages of the latter assay lie in the speed and ease of analysis and interpretation of results. Both tests require confirmatory imaging or further diagnostics, so speeding up the primary triage step can get patients into the correct treatment pathway faster.

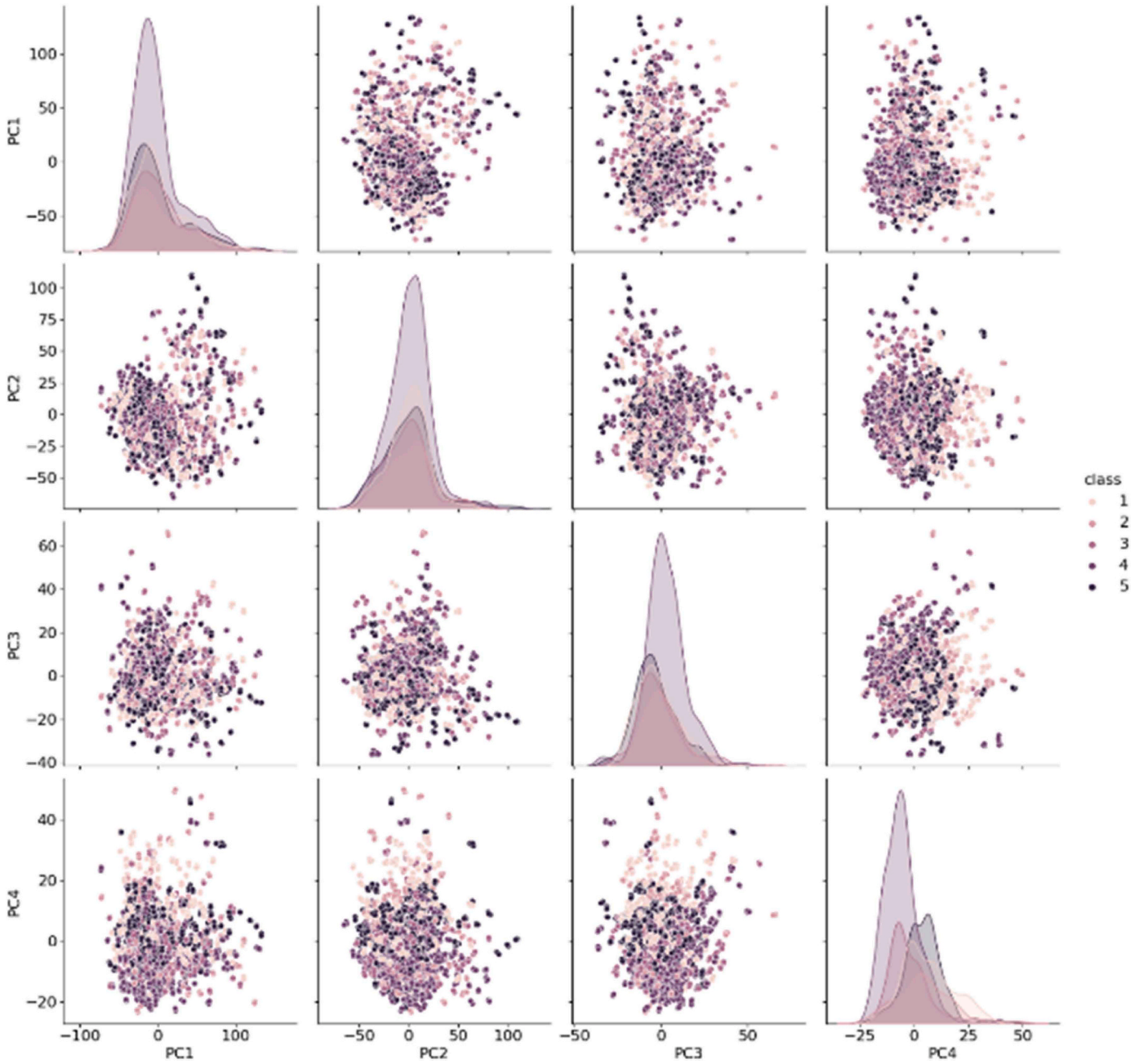

Fig. 2. Principal component analysis scores plot of all disease classes showing the cumulative variance across PC1-PC4, with PC density plots. Group 1 = Heart Failure (ischaemic cardiomyopathy), 2 = Heart Failure No Coronary Artery Disease (non- ischaemic cardiomyopathy), 3 = Symptomatic Controls (coronary artery disease without heart failure), 4 = Healthy Controls, 5 = Heart Failure (atrial fibrillation).

Table 3
Area under the receiver operating curve (AUC), sensitivity and specificity obtained using the oblique random forest partial least squares (ORFPLS) model for prediction of the test set for each classification reported. The statistics are averages over 51 resamples.

Classification	AUC	Sensitivity (%)	Specificity (%)
HF vs Healthy	0.89	80.0	84.1
HF vs SC	0.74	64.0	71.4
HFNOCAD vs Healthy	0.85	75.5	79.6
HFNOCAD vs SC	0.74	80.4	52.4
HF vs Healthy and SC	0.82	75.1	77.1

Table 4
Corresponding sensitivity and specificity values when alternate metric is set to 90%.

Classification	Sensitivity (%) (At 90% Specificity)	Specificity (%) (At 90% Sensitivity)
HF vs Healthy	66	50
HF vs SC	36	23
HFNOCAD vs Healthy	69	48
HFNOCAD vs SC	32	33
HF vs Healthy and SC	60	42

Table 5
Sensitivities and specificities when corresponding metric is set at a minimum of 45%.

Classification problem	Sensitivity (%) (at 45% specificity)	Specificity (%) (at 45% sensitivity)
HF vs Healthy	92	97
HF vs SC	82	86
HFNOCAD vs Healthy	91	97
HFNOCAD vs SC	84	86
HF vs Healthy and SC	89	96

4. Conclusions

Rapid diagnosis of heart failure is vital for improving patient outcomes, as well as reducing cost and streamlining the patient pathway. The current method of a quantitative blood test prior to further diagnostics provide a good NPV, however the pathway could be improved in both cost and time by using the Dxcover liquid biopsy in the primary triage step. This method yields an NPV between 0.94 and 0.99, an AUC of 0.82 with a sensitivity of 45% and a specificity of 96% or when tuned to 45% specificity, sensitivity is 89% and NPV is between 0.97 and 0.99 when assessing the heart failure patients vs healthy controls along with symptomatic controls. The results of this proof-of-concept show promise however further analysis in the form of a full-scale clinical trial would be required to fully assess the assay performance and applicability for implementation into the current pathway.

CRediT authorship contribution statement

Loren Christie: Conceptualization, Methodology, Formal analysis, Visualisation, Writing – original draft, Writing – review & editing. **Alexandra Sala:** Conceptualisation, Methodology, Visualisation, Writing – review & editing. **James M. Cameron:** Conceptualisation, Methodology, Investigation, Writing – review & editing. **Justin J. A. Conn:** Software, Formal analysis. **David S. Palmer:** Software, Supervision, Writing – review & editing. **William J. McGeown**: Conceptualization, Project administration, Review and editing. **Matthew J. Baker:** Conceptualization, Methodology, Writing – review & editing, Project administration, Supervision, Funding Acquisition. **Jane Cannon:** Investigation and Resources. **John Sharp:** Investigation and Resources.

Table 6
Negative Predictive Value at differing prevalence based on age demographics.

Age range	Prevalence of HF (%)	NPV at high sensitivity	NPV at high specificity
All adults [26]	1.5	0.996	0.991
> 65 [27]	5.5	0.986	0.968
> 70 [26]	10	0.974	0.940

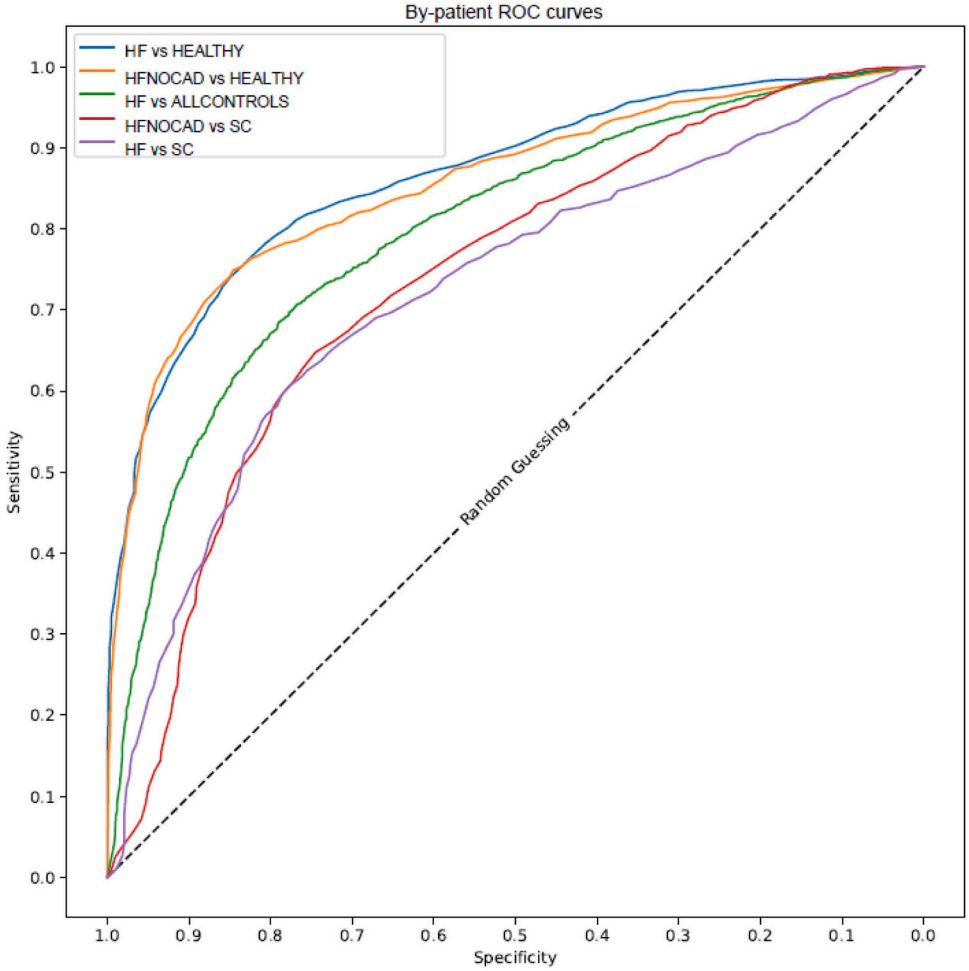

Fig. 3. Receiving operator characteristic curves detailing the trade-off between sensitivity and specificity for all 5 classification problems. Heart failure (NOCAD) vs Healthy patients (blue), Heart failure (NOCAD) vs Symptomatic patients (purple), Heart failure (ISCM and AF) vs Healthy (yellow), Heart failure (ISCM and AF) vs Symptomatic (red) and Heart failure vs Healthy and symptomatic patients (green).

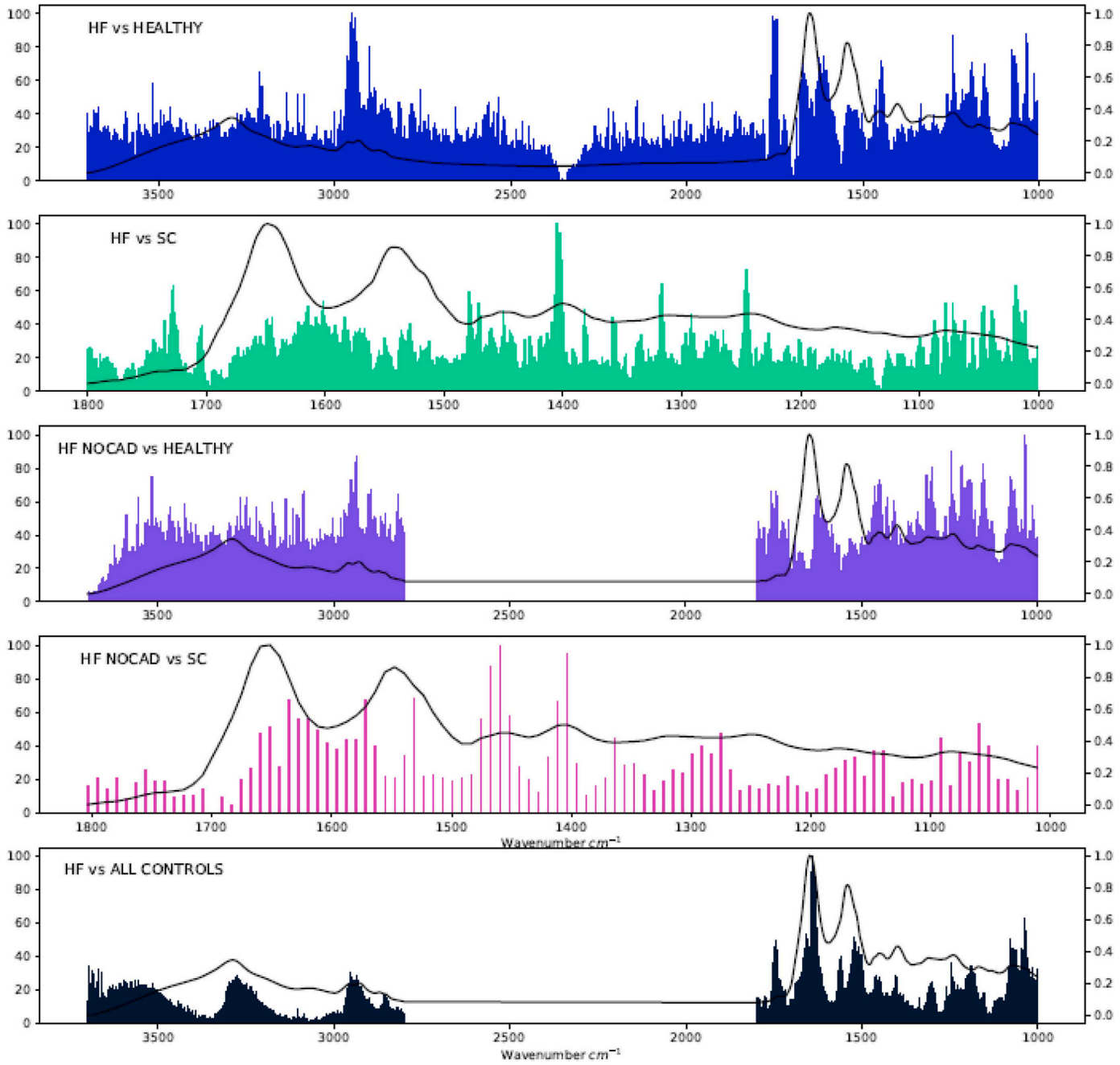

Fig. 4. Feature importance plots generated from the oblique random forest partial least squares (ORFPLS) model for each classification based on the optimum preprocessing for each problem. Preprocessing utilised in each classification can be found in Table 2.

Declaration of Competing Interest

The authors declare the following financial interests/personal relationships which may be considered as potential competing interests: Professor Matthew J Baker and Dr David Palmer are both directors at Dxcover Ltd.

Data availability

The authors do not have permission to share data.

Acknowledgement

The authors would like to thank Dxcover Ltd. and the EPSRC (EP/L505080/1) for funding. The authors would also like to thank Professor John McMurray of the BHF Cardiovascular Research Centre for access to the samples used in this study.

Appendix A. Supporting information

Supplementary data associated with this article can be found in the online version at doi:10.1016/j.clispe.2023.100029.

References

[1] 'Heart failure projected to increase dramatically, according to new statistics', www.heart.org. ⟨https://www.heart.org/en/news/2018/05/01/heart-failure-projected-to-increase-dramatically-according-to-new-statistics⟩ (accessed Jan. 13, 2023).

[2] 'Cardiovascular diseases (CVDs) - WHO'. ⟨https://www.who.int/en/news-room/fact-sheets/detail/cardiovascular-diseases-(cvds)⟩ (accessed Jul. 08, 2020).
[3] S.L. Haas, et al., Spectroscopic diagnosis of myocardial infarction and heart failure by Fourier transform infrared spectroscopy in serum samples, Appl. Spectrosc. vol. 64 (3) (2010) 262–267, https://doi.org/10.1366/000370210790918508.
[4] 'Coronary heart disease - NHS'. ⟨https://www.nhs.uk/conditions/coronary-heart-disease/⟩ (accessed Jul. 08, 2020).
[5] 'Heart failure - NHS'. ⟨https://www.nhs.uk/conditions/heart-failure/⟩ (accessed Jul. 08, 2020).
[6] 'Atrial fibrillation - NHS'. ⟨https://www.nhs.uk/conditions/atrial-fibrillation/⟩ (accessed Jul. 08, 2020).
[7] G.A. Roth, et al., Global burden of cardiovascular diseases and risk factors, 1990–2019, J. Am. Coll. Cardiol. vol. 76 (25) (2020) 2982–3021, https://doi.org/10.1016/j.jacc.2020.11.010.
[8] CDC, 'Heart Disease Facts | cdc.gov', *Centers for Disease Control and Prevention*, Oct. 14, 2022. ⟨https://www.cdc.gov/heartdisease/facts.htm⟩ (accessed Jan. 13, 2023).
[9] 'Heart failure - Diagnosis - NHS'. ⟨https://www.nhs.uk/conditions/heart-failure/diagnosis/⟩ (accessed Jul. 08, 2020).
[10] 'Coronary heart disease - Diagnosis - NHS'. ⟨https://www.nhs.uk/conditions/coronary-heart-disease/diagnosis/⟩ (accessed Jul. 08, 2020).
[11] 'Recommendations | Chronic heart failure in adults: diagnosis and management | Guidance | NICE', Sep. 12, 2018. ⟨https://www.nice.org.uk/guidance/ng106/chapter/Recommendations#diagnosing-heart-failure⟩ (accessed Jul. 05, 2023).
[12] E. Roberts, et al., The diagnostic accuracy of the natriuretic peptides in heart failure: systematic review and diagnostic meta-analysis in the acute care setting, pp. h910–h910, BMJ vol. 350 (mar04 22) (2015), https://doi.org/10.1136/bmj.h910.
[13] M. Ledwidge, et al., Natriuretic peptide–based screening and collaborative care for heart failure: the STOP-HF randomized trial, JAMA vol. 310 (1) (2013) 66–74, https://doi.org/10.1001/jama.2013.7588.
[14] 'Coronary heart disease - Symptoms - NHS'. ⟨https://www.nhs.uk/conditions/coronary-heart-disease/symptoms/⟩ (accessed Jul. 08, 2020).
[15] R. Alizadehsani, et al., Machine learning-based coronary artery disease diagnosis: a comprehensive review, Aug. 01, in: Computers in Biology and Medicine, vol. 111, Elsevier Ltd, 2019, https://doi.org/10.1016/j.compbiomed.2019.103346.
[16] J.H. Joloudari, et al., Coronary artery disease diagnosis; ranking the significant features using a random trees model, Int. J. Environ. Res. Public Health vol. 17 (3) (2020) 731, https://doi.org/10.3390/ijerph17030731.
[17] J. Shaw, F. Rudzicz, T. Jamieson, A. Goldfarb, Artificial intelligence and the implementation challenge, J. Med. Internet Res. vol. 21 (7) (2019), https://doi.org/10.2196/13659.
[18] L.V. Bel'skaya, Use of IR spectroscopy in cancer diagnosis. A review, J. Appl. Spectrosc. vol. 86 (2) (2019) 187–205, https://doi.org/10.1007/s10812-019-00800-w.
[19] M. Paraskevaidi, et al., Differential diagnosis of Alzheimer's disease using spectrochemical analysis of blood, Proc. Natl. Acad. Sci. vol. 114 (38) (2017) E7929–E7938, https://doi.org/10.1073/pnas.1701517114.
[20] A. Sala, et al., Biofluid diagnostics by FTIR spectroscopy: a platform technology for cancer detection, Cancer Lett. vol. 477 (2020) 122–130, https://doi.org/10.1016/j.canlet.2020.02.020.
[21] H.J. Butler, et al., Development of high-throughput ATR-FTIR technology for rapid triage of brain cancer, Nat. Commun. vol. 10 (1) (2019) 1–9, https://doi.org/10.1038/s41467-019-12527-5.
[22] E. Gray, et al., Health economic evaluation of a serum-based blood test for brain tumour diagnosis: exploration of two clinical scenarios, BMJ Open vol. 8 (5) (2018), e017593, https://doi.org/10.1136/bmjopen-2017-017593.
[23] B.R. Smith, M.J. Baker, D.S. Palmer, PRFFECT: a versatile tool for spectroscopists, Chemom. Intell. Lab. Syst. vol. 172 (2018) 33–42, https://doi.org/10.1016/j.chemolab.2017.10.024.
[24] R.J. Hendriks, et al., Clinical use of the SelectMDx urinary-biomarker test with or without mpMRI in prostate cancer diagnosis: a prospective, multicenter study in biopsy-naïve men, Art. no. 4, Prostate Cancer Prostatic Dis. vol. 24 (4) (2021), https://doi.org/10.1038/s41391-021-00367-8.
[25] J. McKiernan, et al., A novel urine exosome gene expression assay to predict high-grade prostate cancer at initial biopsy, JAMA Oncol. vol. 2 (7) (2016) 882–889, https://doi.org/10.1001/jamaoncol.2016.0097.
[26] T.A. McDonagh, et al., 2021 ESC guidelines for the diagnosis and treatment of acute and chronic heart failure: developed by the task force for the diagnosis and treatment of acute and chronic heart failure of the european society of cardiology (ESC) with the special contribution of the heart failure association (HFA) of the ESC', Eur. Heart J. vol. 42 (36) (2021) 3599–3726, https://doi.org/10.1093/eurheartj/ehab368.
[27] P.M. Seferović, et al., The heart failure association atlas: rationale, objectives, and methods, Eur. J. Heart Fail. vol. 22 (4) (2020) 638–645, https://doi.org/10.1002/ejhf.1768.
[28] C.M. Skeaff, J. Miller, Dietary fat and coronary heart disease: summary of evidence from prospective cohort and randomised controlled trials, Ann. Nutr. Metab. vol. 55 (1/3) (2009) 173–201.
[29] M.J. Baker, et al., Using Fourier transform IR spectroscopy to analyze biological materials, Art. no. 8, Nat. Protoc. vol. 9 (8) (2014), https://doi.org/10.1038/nprot.2014.110.